Evaluation of inter-batch differences in stem-cell derived neurons

CrossMark

Gladys Morrison [a,1], Cong Liu [b,1], Claudia Wing [c], Shannon M. Delaney [c], Wei Zhang [d,*], M. Eileen Dolan [a,c,**]

[a] Committee on Clinical Pharmacology and Pharmacogenomics, The University of Chicago, Chicago, IL 60637, USA
[b] Department of Bioengineering, University of Illinois at Chicago, Chicago, IL 60612, USA
[c] Section of Hematology/Oncology, Department of Medicine, The University of Chicago, Chicago, IL 60637, USA
[d] Department of Preventive Medicine & The Robert H. Lurie Comprehensive Cancer Center, Northwestern University Feinberg School of Medicine, Chicago, IL 60611, USA

ARTICLE INFO

ABSTRACT

Differentiated cells retain the genetic information of the donor but the extent to which phenotypic differences between donors or batches of differentiated cells are explained by variation introduced during the differentiation process is not fully understood. In this study, we evaluated four separate batches of commercially available neurons originating from the same iPSCs to investigate whether the differentiation process used in manufacturing iPSCs to neurons affected genome-wide gene expression and modified cytosines, or neuronal sensitivity to drugs. No significant changes in gene expression, as measured by RNA-Seq, or cytosine modification levels, as measured by the Illumina 450K arrays, were observed between batches relative to changes over time. As expected, neurotoxic chemotherapeutics affected neuronal outgrowth, but no inter-batch differences were observed in sensitivity to paclitaxel, vincristine and cisplatin. As a testament to the utility of the model for studies of neuropathy, we observed that genes involved in neuropathy had relatively higher expression levels in these samples across different time points. Our results suggest that the process used to differentiate iPSCs into neurons is consistent, resulting in minimal intra-individual variability across batches. Therefore, this model is reasonable for studies of human neuropathy, druggable targets to prevent neuropathy, and other neurological diseases.

1. Introduction

Neurodegenerative diseases and neuropathy are difficult to study due to lack of relevant human models (Phillips et al., 2009). Cell culture systems and primary rodent cultures have proven to be indispensable to clarify disease mechanisms and provide insights into gene functions. However, the current models have not provided much in terms of therapy for inherited neuropathies (known collectively as Charcot–Marie-Tooth disease) (Ekins et al., 2015), and the only effective treatments for diabetic neuropathy are glucose control and pain management (Callaghan et al., 2012). Chemotherapy-induced peripheral neuropathy (CIPN) is a common neurotoxicity affecting 20–40% of patients receiving chemotherapy (Smith et al., 2013). To truly understand and find relevant druggable targets that are causative, a cellular model that represents neuropathy is essential.

With recent advances in stem cell technology, the ability to differentiate human induced pluripotent stem cells (iPSCs) to neurons provides us with a new and potentially relevant human neuronal model. In addition, iPSC-differentiated neurons can be created from diseased individuals or individuals with severe sensitivity to neurotoxic chemotherapy to provide a model that will allow for the identification of *in vitro* phenotypic characteristics relevant to the disease or sensitivity to neurotoxic drug. These neurons may yield targets essential to overcoming and preventing symptoms associated with heritable neuropathy or CIPN. Stem cell technology has revolutionized the field of "in vitro disease modeling" (Sandoe and Eggan, 2013), as evidenced by the first set of drugs emerging into clinical trials from the use of iPSC derived neurons from patients with neurological diseases (Mullard, 2015).

Human fibroblasts were reprogrammed from an individual into nociceptor neurons without creation of iPSCs and the neurons exhibited sensitization to the chemotherapeutic drug oxaliplatin, modeling the inherent mechanisms underlying painful CIPN (Wainger et al., 2015); however, the advantage to creating iPSCs as an intermediate is that they can grow indefinitely, thus providing a ready source to create additional neurons of the same genetic background. Recently, our laboratory developed a potential model to evaluate CIPN by employing commercially available human neurons differentiated from iPSCs (Wheeler et al., 2015). We found reproducible differences in morphological characteristics including neurite outgrowth phenotypes, cellular viability and apoptosis following treatment with four distinct chemotherapeutic drugs: vincristine, paclitaxel, cisplatin and hydroxyurea. This

* Correspondence to: W. Zhang, 680 N. Lake Shore Dr., Suite 1400, Chicago, IL, 60611, USA.
** Correspondence to: M.E. Dolan, 900 E. 57th St, KCBD 7100, University of Chicago, Chicago, IL 60637, USA.
E-mail addresses: wei.zhang1@northwestern.edu (W. Zhang), edolan@medicine.bsd.uchicago.edu (M.E. Dolan).
[1] These authors contributed equally to this work.

model was also used to demonstrate functional consequences of gene knockdown on neuronal sensitivity to chemotherapeutics of genes identified through clinical genome-wide association studies (GWAS) of CIPN (Wheeler et al., 2015; Leandro-Garcia et al., 2012; Diouf et al., 2015; Komatsu et al., 2015).

The potential of using the human iPSC-derived neuron model for larger genetic association studies requires an understanding of heterogeneity of cultures and to partition the variance associated with iPSC reprograming, culturing, and differentiation (Boulting et al., 2011; Rouhani et al., 2014; Thomas et al., 2015). A major concern in the field of stem cell technology is that techniques to reprogram cells could introduce variation that masks important genetic differences between individuals. A recent study demonstrated that the genetic background of iPSCs generated from peripheral blood mononuclear cells or fibroblasts accounted for more of the variation in gene expression between iPSC lines than any other tested factors such as cell type of origin or reprogramming method (Rouhani et al., 2014). These studies suggest that future studies should focus on collecting a large number of donors rather than generating large numbers of lines from the same donor. Since industrial grade cells can now be made, the evaluation of epigenetics, gene expression and phenotypic variation from batch to batch is an important consideration.

In this study, we obtained multiple batches of iCell® Neurons (iPSC-derived human cortical neurons) differentiated from a single iPSC originating from fibroblasts of an individual to evaluate inter-batch differences in gene expression, cytosine modification levels, and pharmacologic response to chemotherapeutics. To determine the utility of these cells for studies of neuropathy and other neurological diseases, we evaluated genes involved in hereditary neuropathy at different time points in culture as neurites were formed. We showed a consistent enrichment of genes with relatively higher expression levels among hereditary neuropathy associated genes over time.

2. Methods

2.1. ICell Neurons

Neurons (iCell Neurons®) were purchased from Cellular Dynamics International (CDI, Madison, WI, USA). iCell Neurons are an ~98% pure (Tuj1+/Nestin−) pan-neuronal population of GABAergic and to a lesser degree glutamatergic neurons produced from human induced pluripotent stem cells. All batches of iCell Neurons are tested for sterility, viability, purity and morphology, and released according to strict manufacturer's standards. Four batches of iCell Neurons (batch numbers: 1366431, 1366825, 1369525, 1362632) were thawed and maintained according to the manufacturer's protocol. Each batch of iCell Neurons was mixed with 3.3 μg/ml laminin (Sigma-Aldrich) prior to seeding on poly-D-lysine coated 96-well Greiner Bio-One plates at a density of 1.33×10^4 cells/well. Approximately 1.1×10^6 neuron cells were pelleted immediately for the 0 h sample by spinning at $300 \times g$ for 10 min and either lysed using Quizol (Qiagen) for RNA extraction or media removed from pellet before storing both samples at −20 °C. For the cell collections to evaluate modified cytosine and gene expression, cells were pelleted at 0, 4, 28, and 76 h and then extracted DNA and RNA.

2.2. Drug preparation and treatment

Paclitaxel (Sigma-Aldrich) was prepared in the semi-dark by dissolving powder in 100% DMSO and filtered to obtain a stock solution of 58.4 mM. Control wells were treated with 0.17% final concentration of DMSO to match drug treatments. Cisplatin (Sigma-Aldrich) was prepared in the semi-dark by dissolving powder in 100% DMSO and filtered to obtain a stock solution of 20 mM. Control wells were treated with 0.2% final concentration of DMSO to match drug treatment. Vincristine

(Sigma-Aldrich) was prepared on ice in the dark by dissolving powder in cold PBS and filtered to obtain a stock solution of 100 mM. Vincristine stocks were each diluted independently then added into the media and onto the cells before proceeding to the next dilution. All stock drugs were serially diluted in media for final dosing concentrations ranging from 0.01 μM to 100 μM, increasing by factors of ten. Cells were plated and 4 h later treated with increasing concentrations of drug for 72 h.

2.3. High content imaging and neurite outgrowth analysis

After drug treatments of 72 h, neurons were stained for 15 min at 37 °C with 1 μg/ml Hoechst 33342 (Sigma-Aldrich) and 2 μg/ml Calcein AM (Molecular Probes, Life Technologies Inc., Carlsbad, CA, USA) then washed twice using dPBS without calcium or magnesium (LifeTechnologies). Imaging was performed at 10× magnification using an ImageXpress Micro (Molecular Devices, LLC, Sunnyvale, CA, USA) at the University of Chicago Cellular Screening Core. Individual cell measurements of total neurite outgrowth (sum of the length of all processes), number of processes and number of branches were calculated using the MetaXpress software Neurite Outgrowth Application Module (Molecular Devices, LLC). At least 500 cells per dose were quantified in triplicate for three independent experiments.

2.4. Nucleic acid isolation

At each time point, DNA was extracted by adding 50 μl per well of tissue digestion buffer (100 mM NaCl, 50 mM Tris 8.0, 100 mM EDTA, 1% SDS) along with 2 mg/ml Proteinase K (Denville Scientific; South Plainfield, NJ, USA). The plate was sealed with parafilm and agitated overnight at 55 °C using 200 RPM in an Innova orbital shaker (Eppendorf; Enfield, CT). The digested cells from each well were combined and DNA extracted with equal volume of phenol: chloroform (Invitrogen), vortexing for 10 min (Lab Vortex-setting of 4) and the samples were centrifuged for 5 min at $14,000 \times g$. The aqueous phase was collected, extracted with equal volume of chloroform and repeated two times. The DNA was precipitated with equal volume 100% ethanol and centrifuged for 10 min at $14,000 \times g$. Two washes with 70% ethanol produced a pellet that was air dried for 10 min at room temperature and finally dissolved in 50 μl of 10 mM Tris (pH 8.0) for 3 days at 4 °C then stored at −80 °C.

RNA isolation was performed after removal of media and addition of 50 μl Qiazol per well plate for 5 min at room temperature to lyse cells. After vigorously pipetting each well several times, each batch was collected and stored for further processing at −80 °C. When all the time points had been collected, the RNA was purified using the Ambion RNA protocol (15596026.PPS), substituting Qiazol as the lysing reagent after consulting with the company. The final pellet was resuspended in 50 μl of RNase-free water, dissolved at 55 °C for 10 min, aliquoted, and stored at −80 °C.

Nucleic acid quantification was performed using the Quibit dye for RNA or dsDNA kits (Molecular Probes, Life Technologies), as per the manufacturer's specifications.

2.5. RNA-Seq and analysis

1 μg RNA from each time point was submitted to the University of Chicago Genomics Core. RNA quality was then checked on the Agilent Bio-analyzer 2100. RNA-Seq libraries were generated in the core using Illumina RS-122-2101 TruSeq® Stranded mRNA LT libraries and the final libraries checked again on the Agilent bio-analyzer 2100, which was followed by sequencing on the Illumina HiSeq2500. High quality sequencing paired-end reads of 100 bp in each (76.4 to ~83.7%) were mapped to the human genome reference (hg19) using TopHat2 (Kim et al., 2013). Estimated genome coverage is 33.6% to ~52.1%. Cufflinks (Trapnell et al., 2010) were then used to quantify gene expression levels of the assembled transcripts. Fragments per kilobase of transcript per

million mapped reads (FPKM) was calculated for each gene. Only genes with FPKM larger than one remained for downstream analysis. The raw RNA-Seq reads have been deposited to the NIH Short Read Archive (accession no. SRP056287).

2.6. 450K array profiling and analysis

1 μg purified DNA from each time point was submitted to the University of Chicago Genomics Core where it was converted with the EZ-96 DNA Methylation™ Kit, as per the manufacturer's protocol, followed by array analysis using the Illumina Infinium HumanMethylation450 BeadChip (450K array) Kit, which interrogates >480,000 CpG sites in the human genome. The β-value (proportion of modified signals) values were quantile-normalized across all samples. CpGs probes that failed 450K profiling (detection $P > 0.01$) in >5% samples were removed from consideration. The manufacturer's annotations for CpGs sites were checked by aligning CpG probes to the human genome reference (hg19) following our previous publication (Moen et al., 2013). The raw 450K array data have been deposited into the NIH Gene Expression Omnibus database (accession no. GSE66330).

2.7. Batch effect evaluation

Since the conventional principal component analysis (PCA) is not effective for identifying batch effects if they are not the largest source of variation, we applied the gPCA method (Reese et al., 2013) to determine whether there was a batch effect observed in the RNA-Seq data and methylation data. Briefly gPCA guides the singular-value decomposition to look for batch effects in the data based on the batch indicator matrix. A statistic δ was derived from the ratio of the variance of the first PC from gPCA to the variance of the first PC from unguided PCA. A larger δ is expected if there exists a batch effect. To determine the significance, an empirical P-value was estimated by permuting the batch vector 1000 times. The percentage of total variance explained by batch was then calculated as a percentage of variance proportion increase of the first PC using guided PCA. In addition, for each gene, we performed a two-way ANOVA test to test the batch effect. False discovery rate (FDR) was estimated using the Benjamini–Hochberg procedure (Benjamini, 1995).

2.8. Evaluation of enrichment of neuropathy-associated genes

Hereditary neuropathy- (48 genes) and diabetes- (27 genes) associated gene lists were downloaded from Online Mendelian Inheritance in Man (OMIM) (accessed on Oct. 30, 2014). In addition, 13 CIPN associated genes were extracted from previous publications (Leandro-Garcia et al., 2012; Seretny et al., 2014; Wheeler et al., 2013; Baldwin et al., 2012; Leandro-Garcia et al., 2013; Li et al., 2014, 2015a; Beutler et al., 2014; Li et al., 2015b; Boora et al., 2015) (Table 1). We further obtained a list of additional neuropathy-associated genes from Reyes-Gibby et al.

(Reyes-Gibby et al., 2015). We calculated the median gene expression levels of neuropathy-associated genes (hereditary neuropathy or CIPN, separately) at each time point. To determine the null distribution of median gene expression, we randomly sampled the same number of genes across whole transcriptome according to the RefSeq annotations (Pruitt et al., 2005). Empirical P-values of enrichment were calculated as the probability of getting at least the median expression value as neuropathy-associated genes under the null distribution. We performed the same analysis with diabetes-associated genes.

3. Results

3.1. Scheme of iPSC differentiation efficiency analysis in cortical neurons

To investigate whether the differentiation process from iPSC to neurons introduces variation in epigenetics and gene expression, we evaluated these parameters in four distinct batches of neurons created from a single iPSC clone from a single individual (Fig. 1, Table 2). iPSC-differentiated cortical neurons are a mixed population of neuronal cells consisting mainly of GABAergic and glutamatergic neurons (Wheeler et al., 2015). These differentiated neurons were shown to be Tuj1 positive with no obvious morphological differences between three neuronal batches imaged at 48 and 72 h after plating (Fig. 1). We evaluated batch effect between lots by analyzing gene expression using RNA-Seq and modified cytosines using the Illumina 450K arrays, as well as temporal changes of these measurements following neuronal plating. These neurons quickly assumed a typical neuronal morphology with branching neurites that can be measured using an imaging system.

3.2. Transcriptomic profiling of different batches of neurons

All four batches of cortical neurons differentiated from iPSCs were analyzed using RNA-Seq at 0, 4, 28 and 76 h following plating. Traditional PCA of the log-transformed FPKM matrix was first plotted for visualization (Fig. 2A). gPCA was then performed to derive statistical conclusions. Permutation test showed that there was no significant batch effect detected among RNA-Seq measurements (δ = 0.49; P-value = 0.93). Of the total variances in gene expression among samples, which is represented by summations of squared deviation from mean value, 71.55% could be explained by temporal changes, while 27.05% of the total variance could be explained by different batches (see details in the Methods section). Therefore, the temporal effect contributes predominantly to the observed variances. The sum of variances derived from these two major sources of variation may not be equal to 1 due to their possible interaction. Notably, two protein-coding genes (*DNASE2B* encoding deoxyribonuclease II beta and *PALMD* encoding palmdelphin) were found to be significant for the batch effect at a lenient cutoff of 20% FDR, with no detection of functional enrichment among batch effect genes. Furthermore, none of the neuropathy-associated genes (Leandro-Garcia et al., 2012; Wheeler et al., 2013;

Table 1
Published CIPN associated genes.

HGNC symbol	Cytogenetic band	Description	References
CX3CL1	16q21	Chemokine (C-X-3-C motif) ligand 1	Li et al. (2015a)
EPHA4	2q36.1	Ephrin receptor A4	Leandro-Garcia et al. (2013)
EPHA5	4q13.2	Ephrin receptor A5	Baldwin et al. (2012), Leandro-Garcia et al. (2013)
EPHA6	3q11.2	Ephrin receptor A6	Leandro-Garcia et al. (2013)
FGD4	12p11.21	FYVE, RhoGEF and PH domain containing 4	Baldwin et al. (2012)
FZD3	8p21.1	Frizzled class receptor 3	Reyes-Gibby et al. (2015)
LIMK2	22q12.2	LIM domain kinase 2	Leandro-Garcia et al. (2013)
PRX	19q13.2	Periaxin	Beutler et al. (2014)
RFX2	19p13.3	Regulatory factor X, 2 (influences HLA class II expression)	Wheeler et al. (2013)
TLR4	9q33.1	Toll-like receptor 4	Li et al. (2014, 2015b)
TUBB2A	6p25.2	Tubulin, beta 2A class IIa	Leandro-Garcia et al. (2012)
XKR4	8q12.1	XK, Kell blood group complex subunit-related family, member 4	Baldwin et al. (2012), Leandro-Garcia et al. (2013)
ARHGEF10	8p23.3	Rho guanine nucleotide exchange factor 10	Beutler et al. (2014), Boora et al. (2015)

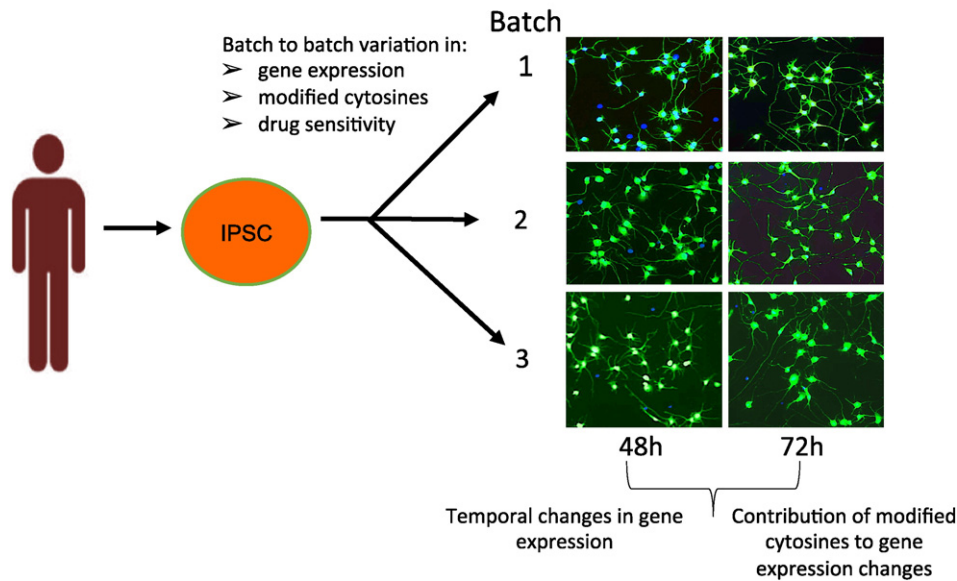## Profiling of iPSC differentiated neurons

Fig. 1. Overall schematic to investigate epigenetic and gene expression differences between batches and following time in culture. Four independent batches of neurons reprogrammed from a single iPSC from a single human fibroblasts were purchased from Cellular Dynamics, Int. These three neuron batches (shown) as well as a fourth batch (not shown) were pelleted to evaluate genome wide gene expression (RNA-Seq) and modified cytosines (Illumina 450K). In the phenotypic assay, three neuron batches out of the four were plated and neurite outgrowth was imaged at 48 and 76 h, using MetaXPress.

Baldwin et al., 2012; Leandro-Garcia et al., 2013; Li et al., 2014, 2015a; Beutler et al., 2014; Li et al., 2015b; Boora et al., 2015; Reyes-Gibby et al., 2015) was significantly (FDR < 0.2) affected by batch.

3.3. Modified cytosine profiling of different batches of neurons

We then analyzed cytosine modification levels using the Illumina 450K arrays for 4 neuron batches at the same 4 different plating time points. PCA plot of the β-value matrix was obtained from the 450K array data (Fig. 2B). gPCA test indicated that no significant batch effect separating the batches ($\delta = 0.44$; P-value $= 0.50$) was detected (Fig. 2B). Similar to the RNA-Seq data, 89.28% of the variance was explained by temporal changes in the 450K array data, while 56.4% of the total variance could be explained by batch. These results suggested that both gene expression and cytosine modification measurements were consistent across different batches but changed as neurites were formed in culture, as expected.

3.4. Phenotypic measures of chemotherapeutic sensitivity of different batches of neurons

We also measured neuronal phenotype (i.e., pharmacologic response to chemotherapy), in three out of four batches of the neurons. Human neurons reprogrammed from fibroblasts have been used to study chemotherapeutics that cause CIPN (Wainger et al., 2015; Wheeler et al., 2015) and genes associated with clinical CIPN (Wheeler et al., 2015; Leandro-Garcia et al., 2012; Diouf et al., 2015; Komatsu et al., 2015). We identified no significant differences between batches in sensitivities to paclitaxel, vincristine and cisplatin as determined by total neurite outgrowth (Fig. 3A), number of processes (Fig. 3B) and branches (Fig. 3C) and as illustrated morphologically for 0, 0.1 and 10 μM paclitaxel (Fig. 3D), vincristine (Fig. 3E) and cisplatin (Fig. 3F).

3.5. Enrichment of highly expressed neuropathy related genes in the neuron model

Tissue-specific models are essential in understanding mechanisms of disease onset and drug induced toxicity, however expression of genes critical to the disease is necessary for the model to be useful. We therefore sought to investigate the degree to which established neuropathy associated genes were enriched in this neuronal cell model. Fig. 4 illustrates the median gene expression levels of neuropathy-associated genes at each time point. In the gene expression data, we found that at each time point (0, 4, 28 and 76 h), hereditary neuropathy related genes from OMIM were highly expressed compared with background distribution across the human genome (empirical P-value < 0.001) (Fig. 4A). In addition, a few known CIPN related genes from previous publications also showed a trend of enrichment of highly expressed genes relative to the background (Fig. 4B, Table 1). To determine if this enrichment was specific to neuropathic disease but not other diseases, we evaluated diabetes-associated genes as a negative control and found no enrichment (Fig. 4C). These results overall suggest that this is a relevant neuronal model to study the pathophysiology of neuropathy.
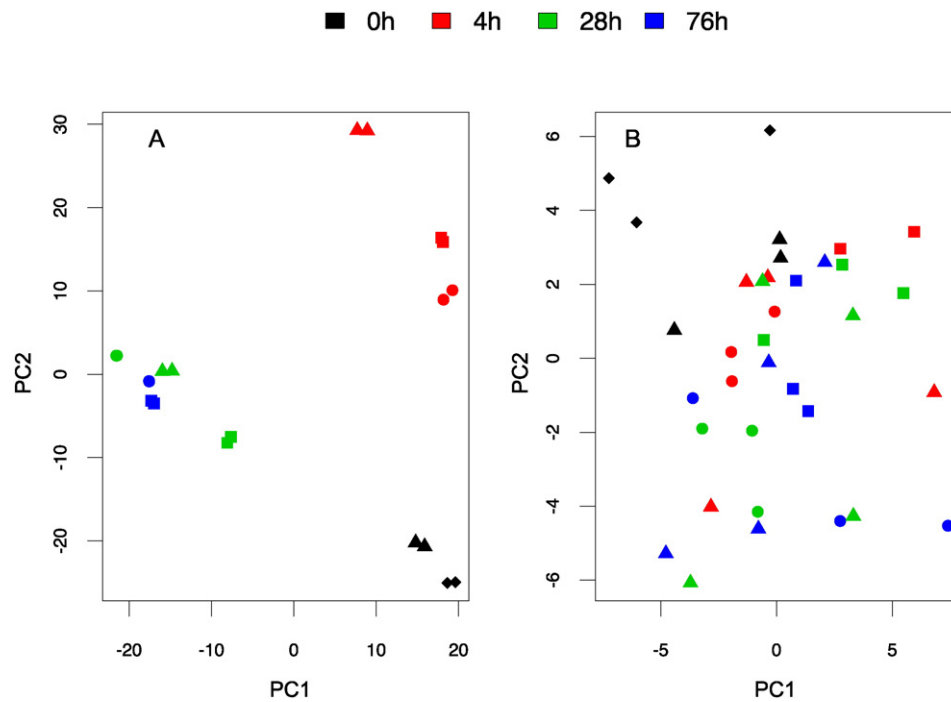
Table 2
Four independently differentiated neurons and the experiments performed with each batch.

Batch # Lot #	Plating time (h)	Number of replicates		
		RNA-Seq	450K assay	Sensitivity assay
1 1369525	4	2	2	3
	28	2	3	–
	76	2	3	–
2 1366825	4	2	3	3
	28	2	3	–
	76	2	3	–
	0	2	3	–
3 1366431	4	2	4	3
	28	2	4	–
	76	–	4	–
4 1362632	0	2	3	–

Fig. 2. Analyzing batch effect using RNA-Seq and Illumina 450K array. Four independent batches of neurons denoted by shapes (square: lot # 1366825, triangle: lot # 1366431, circle: lot # 1369525 and diamond: lot # 1362632) were collected at different time points (0, 4, 28, 76 h) denoted by color. Lot # 1362632 had pellets collected only at time point 0. A) A PCA plot of the log-transformed RNA-Seq data in FPKM (fragments per kilobase of transcript per million mapped reads); B) a PCA plot of the β-values from the Illumina 450K array. PC1: the first principal component; PC2: the second principal component.

4. Discussion

We evaluated inter-batch variability of differentiated neurons in order to provide insight into variability associated with manufacturing neurons from iPSCs (i.e., the differentiation process). It is important to consider the magnitude of noise introduced by processing the cells relative to biological signal. High quality and stable iPSC-derived neurons depend on the robustness of the manufacturing protocol for both the iPSC-differentiated cells and the production of the iPSCs themselves (Ohnuki et al., 2014). Such standards of quality are most practically achieved by large core facilities and commercial manufacturers.

In our study, four independent productions of iCell Neurons were obtained from CDI; each production represents an independent differentiation from the same iPSC clone. We found through RNA-Seq analysis that gene expression variation due to different batches was not a major source of variance compared to changes over time. Modified cytosine changes also showed no significant variation across batches as compared to time dependent changes suggesting that the differentiation process results in minimal intra-individual variation. The lack of significant variation of neuronal sensitivity to neurotoxic chemotherapeutics for 3 separate batches provided further confidence that inter-batch variation is minimal. We next investigated whether the iPSC-derived neuronal model system is adequately enriched for the genes essential in identifying mechanisms of neuronal diseases and drug-induced neurotoxicities. Indeed, we found that the neurons were enriched for highly expressed genes implicated in hereditary neuropathy and showed an enrichment trend for a few genes known to be associated with chemotherapeutic-induced neuropathy. The lack of significance of CIPN related genes may be because of our limited knowledge of genes contributing to CIPN. The specificity of our model was further confirmed when we found that our model was not enriched for genes implicated in other disease types, such as diabetes.

An advantage of the creation of patient-derived iPSCs is that they retain the genetic "makeup" of the donor allowing for *in vitro* studies of neurons from patients with specific diseases that harbor the complex genetic background associated with the disorder (Ohnuki et al., 2014). The successful generation of iPSCs from patients' specific somatic cells,

and differentiation to cortical neurons, have offered cell resources for disease modeling and potential cell transplantation therapy (Corti et al., 2015). This revolutionary technology has already helped to advance our understanding of many diseases and inform mechanistically rationalized therapies, which are desperately needed in this arena (Mullard, 2015; Wiethoff et al., 2015).

Charcot–Marie tooth (CMT) is one of the most common inherited neurological disorders, characterized by weakness of the foot and lower leg muscle (Newman et al., 2007) and has no effective treatment. Therefore, human iPSCs can lead to the identification and optimization of potential drugs and thus move forward new pharmacological therapies for a wide range of neurodegenerative and neurodevelopmental conditions (Corti et al., 2015). Critical to this field is the consistent manufacturing of differentiated neurons from iPSCs. Therefore, our evaluation of gene expression and modified cytosines at baseline, and changes over time following plating, will provide a framework for studies of these neurons. Furthermore, we show batch-to-batch consistency of iPSC-derived neurons in gene expression, modified cytosines and response to neurotoxic chemotherapeutics.

Creating a genetically diverse set of differentiated cells for the purposes of phenotype-genotype studies would have great value in pharmacogenomics, a field that has relied primarily on EBV-transformed lymphoblastoid cell lines (Moen et al., 2012; Wheeler and Dolan, 2012; Welsh et al., 2009). Tissue specific cells will provide the appropriate model for functionally validating findings from large clinical genome wide association studies. Therefore, the development of human iPSC-derived neurons as a model system could have important implications for studies of neurotoxicity and developing new drugs to prevent or treat heritable neuropathy and/or CIPN, one of the most common and sometimes permanent side effects of chemotherapy (Alberti et al., 2014; Cavaletti et al., 2013).

5. Conclusion

Our results indicate that batch-to-batch variation in gene expression, modified cytosines and drug sensitivity was not a major source
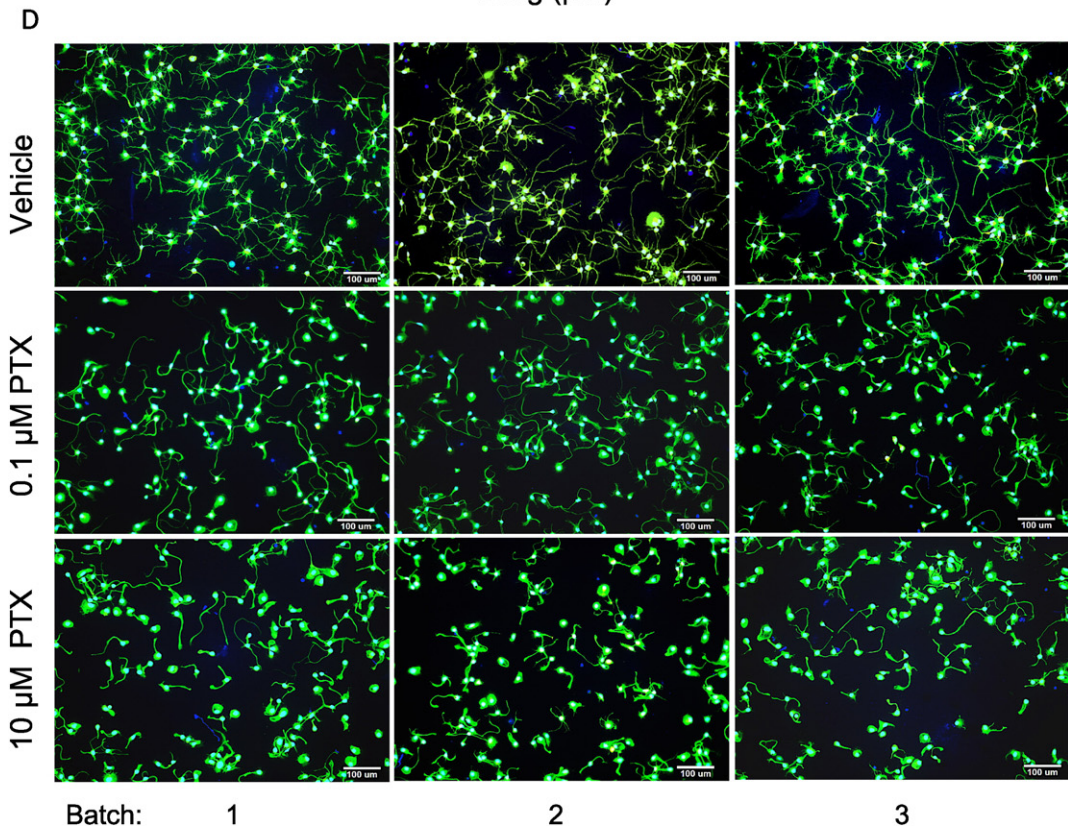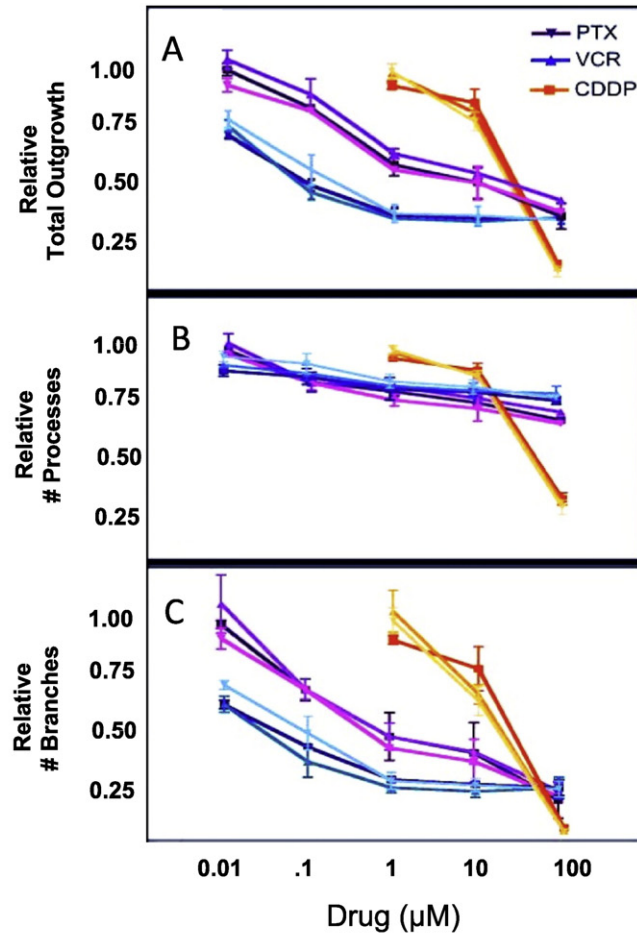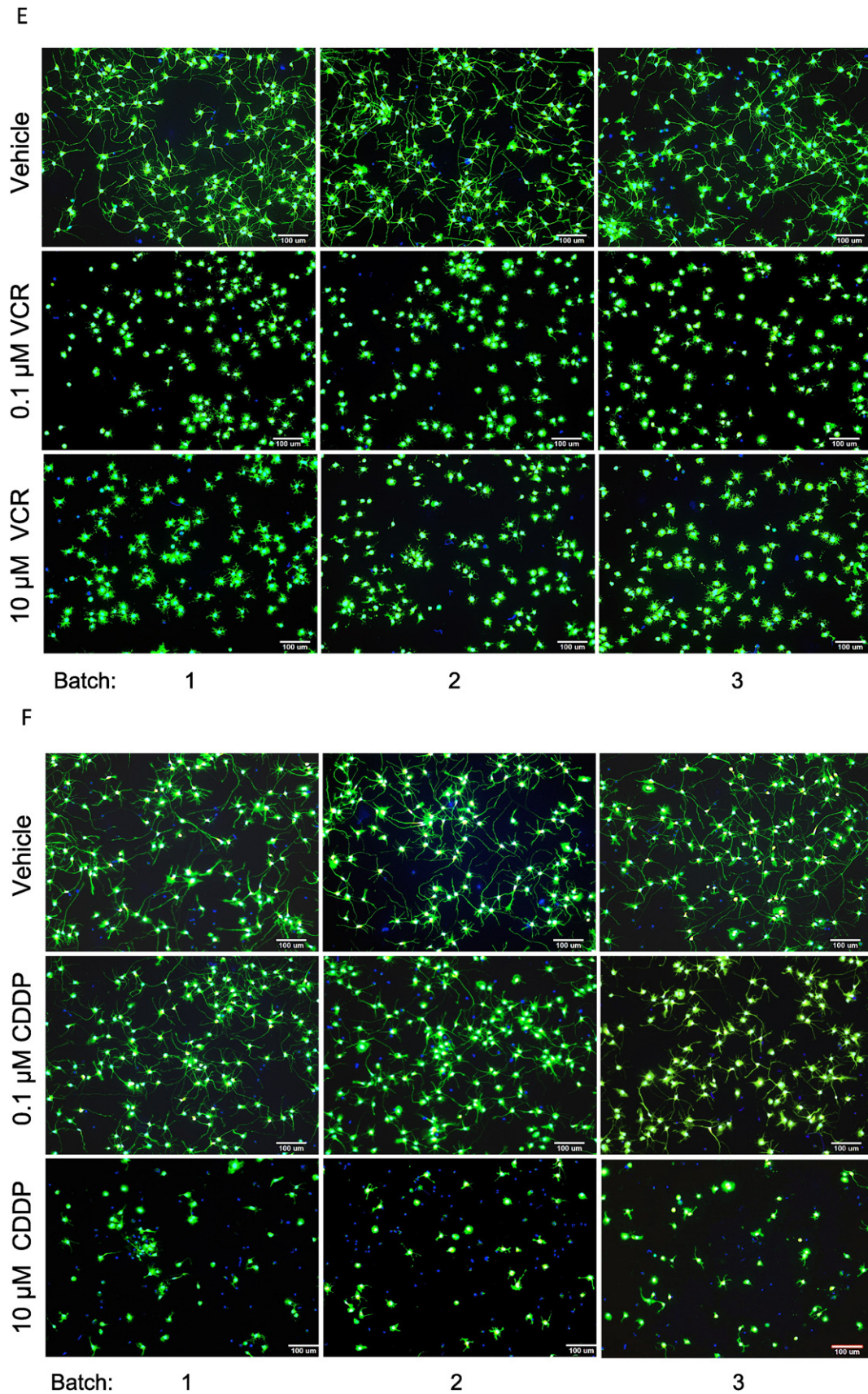
Fig. 3. Effect of chemotherapeutic agents on neuronal outgrowth. Three batches of iCell Neurons out of the four batches were treated with increasing concentrations of paclitaxel (PTX, purple), vincristine (VCR, blue) or cisplatin (CDDP, orange) for 72 h, and analyzed with the MetaXPress software for (A) relative total outgrowth; (B) relative number of processes; and (C) relative number of branches. The three batches are represented as shaded differences in color for each drug response curve (lightest shade: lot # 1369525; medium shade: lot # 1366825 and darkest shade: lot # 1366431). Representative 10× images of 3 batches iCell Neurons treated with different concentrations of vehicle (DMSO or PBS), 0.1 μM or 10 μM of (D) PTX, (E) VCR and (F) CDDP at 72 h using ImageXpress Micro.
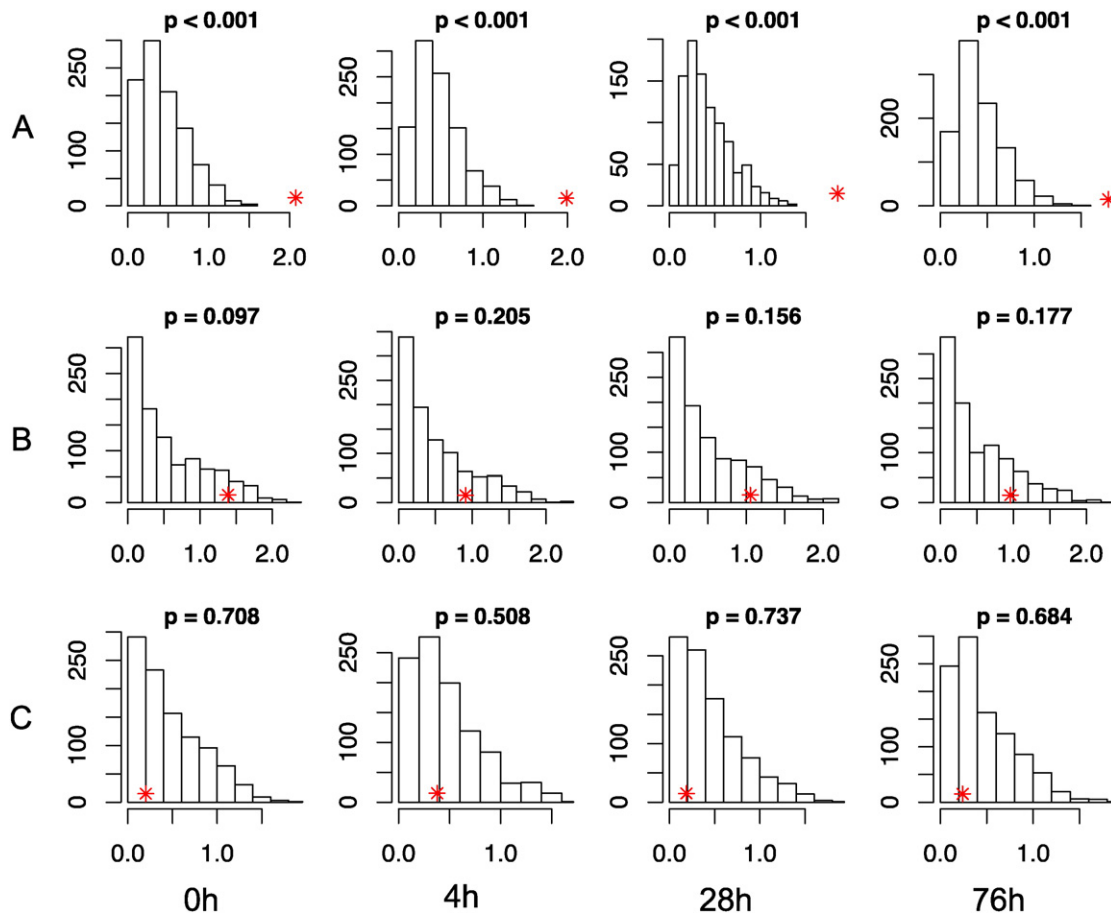
Fig. 4. Assessing enrichment of neuropathy associated genes in neuronal model. Median gene expression levels measured as log FPKM (X-axis) of: A) hereditary neuropathy-; B) CIPN-; and C) diabetes-associated genes at each time point are indicated by red asterisks. The histograms show the null distributions (frequencies on the Y-axis) generated by random samplings of the same number of genes across the human genome. Empirical *P*-values are indicated for each situation. CIPN: chemotherapy-induced peripheral neuropathy; FPKM: fragments per kilobase of transcript per million mapped reads.

of variances compared to the time effect. The enrichment of neuropathy associated genes in the neurons in contrast to other diseases such as diabetes, gives us a clinically relevant cell-based model that will allow us to understand the mechanisms of neurological disease and drug induced neurotoxicities. This model also provides a flexible platform to test potential neurotoxic and/or neuroprotectant drugs.

Author contributions

Gladys Morrison: Collection and/or assembly of data, data analysis and interpretation, manuscript writing.

Cong Liu: Data analysis and interpretation, manuscript writing.

Claudia Wing: Collection and/or assembly of data, data analysis and interpretation, manuscript writing (Methods section).

Shannon M Delaney: Collection and/or assembly of data.

Wei Zhang: Conception and design, financial support, collection and/or assembly of data, data analysis and interpretation, manuscript writing, final approval of manuscript.

M. Eileen Dolan: Conception and design, financial support, collection and/or assembly of data, data analysis and interpretation, manuscript writing, final approval of manuscript.

Disclosure of potential conflict of interest

The authors do not have any potential conflict of interest.

References

Alberti, P., Rossi, E., Cornblath, D.R., Merkies, I.S., Postma, T.J., Frigeni, B., Bruna, J., Velasco, R., Argyriou, A.A., Kalofonos, H.P., Psimaras, D., Ricard, D., Pace, A., Galie, E., Briani, C., Dalla Torre, C., Faber, C.G., Lalisang, R.I., Boogerd, W., Brandsma, D., Koeppen, S., Hense, J., Storey, D., Kerrigan, S., Schenone, A., Fabbri, S., Valsecchi, M.G., Cavaletti, G., C.I.-P. Group, 2014. Physician-assessed and patient-reported outcome measures in chemotherapy-induced sensory peripheral neurotoxicity: two sides of the same coin. Ann. Oncol. 25, 257–264.

Baldwin, R.M., Owzar, K., Zembutsu, H., Chhibber, A., Kubo, M., Jiang, C., Watson, D., Eclov, R.J., Mefford, J., McLeod, H.L., Friedman, P.N., Hudis, C.A., Winer, E.P., Jorgenson, E.M., Witte, J.S., Shulman, L.N., Nakamura, Y., Ratain, M.J., Kroetz, D.L., 2012. A genome-wide association study identifies novel loci for paclitaxel-induced sensory peripheral neuropathy in CALGB 40101. Clin. Cancer Res. 18, 5099–5109.

Benjamini, Y., 1995. Hotchberg, Y, Controlling the false discovery rate: a practical and powerful approach to multiple testing. J. R. Stat. Soc. Ser. B Methodol. 51, 289–300.

Beutler, A.S., Kulkarni, A.A., Kanwar, R., Klein, C.J., Therneau, T.M., Qin, R., Banck, M.S., Boora, G.K., Ruddy, K.J., Wu, Y., Smalley, R.L., Cunningham, J.M., Le-Lindqwister, N.A., Beyerlein, P., Schroth, G.P., Windebank, A.J., Zuchner, S., Loprinzi, C.L., 2014.

Sequencing of Charcot–Marie-tooth disease genes in a toxic polyneuropathy. Ann. Neurol. 76, 727–737.

Boora, G.K., Kulkarni, A.A., Kanwar, R., Beyerlein, P., Qin, R., Banck, M.S., Ruddy, K.J., Pleticha, J., Lynch, C.A., Behrens, R.J., Zuchner, S., Loprinzi, C.L., Beutler, A.S., 2015. Association of the Charcot–Marie-tooth disease gene ARHGEF10 with paclitaxel induced peripheral neuropathy in NCCTG N08CA (Alliance). J. Neurol. Sci.

Boulting, G.L., Kiskinis, E., Croft, G.F., Amoroso, M.W., Oakley, D.H., Wainger, B.J., Williams, D.J., Kahler, D.J., Yamaki, M., Davidow, L., Rodolfa, C.T., Dimos, J.T., Mikkilineni, S., MacDermott, A.B., Woolf, C.J., Henderson, C.E., Wichterle, H., Eggan, K., 2011. A functionally characterized test set of human induced pluripotent stem cells. Nat. Biotechnol. 29, 279–286.

Callaghan, B.C., Cheng, H.T., Stables, C.L., Smith, A.L., Feldman, E.L., 2012. Diabetic neuropathy: clinical manifestations and current treatments. Lancet Neurol. 11, 521–534.

Cavaletti, G., Cornblath, D.R., Merkies, I.S., Postma, T.J., Rossi, E., Frigeni, B., Alberti, P., Bruna, J., Velasco, R., Argyriou, A.A., Kalofonos, H.P., Psimaras, D., Ricard, D., Pace, A., Galie, E., Briani, C., Dalla Torre, C., Faber, C.G., Lalisang, R.I., Boogerd, W., Brandsma, D., Koeppen, S., Hense, J., Storey, D., Kerrigan, S., Schenone, A., Fabbri, S., Valsecchi, M.G., C.I.-P. Group, 2013. The chemotherapy-induced peripheral neuropathy outcome measures standardization study: from consensus to the first validity and reliability findings. Ann. Oncol. 24, 454–462.

Corti, S., Faravelli, I., Cardano, M., Conti, L., 2015. Human pluripotent stem cells as tools for neurodegenerative and neurodevelopmental disease modeling and drug discovery. Expert Opin. Drug Discovery 10, 615–629.

Diouf, B., Crews, K.R., Lew, G., Pei, D., Cheng, C., Bao, J., Zheng, J.J., Yang, W., Fan, Y., Wheeler, H.E., Wing, C., Delaney, S.M., Komatsu, M., Paugh, S.W., McCorkle, J.R., Lu, X., Winick, N.J., Carroll, W.L., Loh, M.L., Hunger, S.P., Devidas, M., Pui, C.H., Dolan, M.E., Relling, M.V., Evans, W.E., 2015. Association of an inherited genetic variant with vincristine-related peripheral neuropathy in children with acute lymphoblastic leukemia. JAMA 313, 815–823.

Ekins, S., Litterman, N.K., Arnold, R.J., Burgess, R.W., Freundlich, J.S., Gray, S.J., Higgins, J.J., Langley, B., Willis, D.E., Notterpek, L., Pleasure, D., Sereda, M.W., Moore, A., 2015. A Brief Review of Recent Charcot–Marie-Tooth Research and Priorities. F1000Res 4 p. 53.

Kim, D., Pertea, G., Trapnell, C., Pimentel, H., Kelley, R., Salzberg, S.L., 2013. TopHat2: accurate alignment of transcriptomes in the presence of insertions, deletions and gene fusions. Genome Biol. 14, R36.

Komatsu, M., Wheeler, H.E., Chung, S., Low, S.K., Wing, C., Delaney, S.M., Gorsic, L.K., Takahashi, A., Kubo, M., Kroetz, D., Zhang, W., Nakamura, Y., Dolan, M.E., 2015. Pharmacoethnicity in paclitaxel-induced sensory peripheral neuropathy. Clin. Cancer Res.

Leandro-Garcia, L.J., Leskela, S., Jara, C., Green, H., Avall-Lundqvist, E., Wheeler, H.E., Dolan, M.E., Inglada-Perez, L., Maliszewska, A., de Cubas, A.A., Comino-Mendez, I., Mancikova, V., Cascon, A., Robledo, M., Rodriguez-Antona, C., 2012. Regulatory polymorphisms in beta-tubulin IIa are associated with paclitaxel-induced peripheral neuropathy. Clin. Cancer Res. 18, 4441–4448.

Leandro-Garcia, L.J., Inglada-Perez, L., Pita, G., Hjerpe, E., Leskela, S., Jara, C., Mielgo, X., Gonzalez-Neira, A., Robledo, M., Avall-Lundqvist, E., Green, H., Rodriguez-Antona, C., 2013. Genome-wide association study identifies ephrin type A receptors implicated in paclitaxel induced peripheral sensory neuropathy. J. Med. Genet. 50, 599–605.

Li, Y., Zhang, H., Zhang, H., Kosturakis, A.K., Jawad, A.B., Dougherty, P.M., 2014. Toll-like receptor 4 signaling contributes to paclitaxel-induced peripheral neuropathy. J. Pain 15, 712–725.

Li, D., Huang, Z.Z., Ling, Y.Z., Wei, J.Y., Cui, Y., Zhang, X.Z., Zhu, H.Q., Xin, W.J., 2015a. Up-regulation of CX3CL1 via nuclear factor-kappaB-dependent histone acetylation is involved in paclitaxel-induced peripheral neuropathy. Anesthesiology 122, 1142–1151.

Li, Y., Zhang, H., Kosturakis, A.K., Cassidy, R.M., Zhang, H., Kennamer-Chapman, R.M., Jawad, A.B., Colomand, C.M., Harrison, D.S., Dougherty, P.M., 2015b. MAPK signaling downstream to TLR4 contributes to paclitaxel-induced peripheral neuropathy. Brain Behav. Immun.

Moen, E.L., Godley, L.A., Zhang, W., Dolan, M.E., 2012. Pharmacogenomics of chemotherapeutic susceptibility and toxicity. Genome Med. 4, 90.

Moen, E.L., Zhang, X., Mu, W., Delaney, S.M., Wing, C., McQuade, J., Myers, J., Godley, L.A., Dolan, M.E., Zhang, W., 2013. Genome-wide variation of cytosine modifications between European and African populations and the implications for complex traits. Genetics 194, 987–996.

Mullard, A., 2015. Stem-cell discovery platforms yield first clinical candidates. Nat. Rev. Drug Discov. 14, 589–591.

Newman, C.J., Walsh, M., O'Sullivan, R., Jenkinson, A., Bennett, D., Lynch, B., O'Brien, T., 2007. The characteristics of gait in Charcot–Marie-tooth disease types I and II. Gait Posture 26, 120–127.

Ohnuki, M., Tanabe, K., Sutou, K., Teramoto, I., Sawamura, Y., Narita, M., Nakamura, M., Tokunaga, Y., Nakamura, M., Watanabe, A., Yamanaka, S., Takahashi, K., 2014. Dynamic regulation of human endogenous retroviruses mediates factor-induced reprogramming and differentiation potential. Proc. Natl. Acad. Sci. U. S. A. 111, 12426–12431.

Phillips, W., Michell, A., Pruess, H., Barker, R.A., 2009. Animal models of neurodegenerative diseases. Methods Mol. Biol. 549, 137–155.

Pruitt, K.D., Tatusova, T., Maglott, D.R., 2005. NCBI Reference Sequence (RefSeq): a curated non-redundant sequence database of genomes, transcripts and proteins. Nucleic Acids Res. 33, D501–D504.

Reese, S.E., Archer, K.J., Therneau, T.M., Atkinson, E.J., Vachon, C.M., de Andrade, M., Kocher, J.P., Eckel-Passow, J.E., 2013. A new statistic for identifying batch effects in high-throughput genomic data that uses guided principal component analysis. Bioinformatics 29, 2877–2883.

Reyes-Gibby, C.C., Wang, J., Yeung, S.C., Shete, S., 2015. Informative gene network for chemotherapy-induced peripheral neuropathy. BioData Min. 8, 24.

Rouhani, F., Kumasaka, N., de Brito, M.C., Bradley, A., Vallier, L., Gaffney, D., 2014. Genetic background drives transcriptional variation in human induced pluripotent stem cells. PLoS Genet. 10, e1004432.

Sandoe, J., Eggan, K., 2013. Opportunities and challenges of pluripotent stem cell neurodegenerative disease models. Nat. Neurosci. 16, 780–789.

Seretny, M., Currie, G.L., Sena, E.S., Ramnarine, S., Grant, R., MacLeod, M.R., Colvin, L.A., Fallon, M., 2014. Incidence, prevalence, and predictors of chemotherapy-induced peripheral neuropathy: a systematic review and meta-analysis. Pain 155, 2461–2470.

Smith, E.M., Pang, H., Cirrincione, C., Fleishman, S., Paskett, E.D., Ahles, T., Bressler, L.R., Fadul, C.E., Knox, C., Le-Lindqwister, N., Gilman, P.B., Shapiro, C.L., 2013. O. Alliance for clinical trials in, effect of duloxetine on pain, function, and quality of life among patients with chemotherapy-induced painful peripheral neuropathy: a randomized clinical trial. JAMA 309, 1359–1367.

Thomas, S.M., Kagan, C., Pavlovic, B.J., Burnett, J., Patterson, K., Pritchard, J.K., Gilad, Y., 2015. Reprogramming LCLs to iPSCs results in recovery of donor-specific gene expression signature. PLoS Genet. 11, e1005216.

Trapnell, C., Williams, B.A., Pertea, G., Mortazavi, A., Kwan, G., van Baren, M.J., Salzberg, S.L., Wold, B.J., Pachter, L., 2010. Transcript assembly and quantification by RNA-Seq reveals unannotated transcripts and isoform switching during cell differentiation. Nat. Biotechnol. 28, 511–515.

Wainger, B.J., Buttermore, E.D., Oliveira, J.T., Mellin, C., Lee, S., Saber, W.A., Wang, A.J., Ichida, J.K., Chiu, I.M., Barrett, L., Huebner, E.A., Bilgin, C., Tsujimoto, N., Brenneis, C., Kapur, K., Rubin, L.L., Eggan, K., Woolf, C.J., 2015. Modeling pain in vitro using nociceptor neurons reprogrammed from fibroblasts. Nat. Neurosci. 18, 17–24.

Welsh, M., Mangravite, L., Medina, M.W., Tantisira, K., Zhang, W., Huang, R.S., McLeod, H., Dolan, M.E., 2009. Pharmacogenomic discovery using cell-based models. Pharmacol. Rev. 61, 413–429.

Wheeler, H.E., Dolan, M.E., 2012. Lymphoblastoid cell lines in pharmacogenomic discovery and clinical translation. Pharmacogenomics 13, 55–70.

Wheeler, H.E., Gamazon, E.R., Wing, C., Njiaju, U.O., Njoku, C., Baldwin, R.M., Owzar, K., Jiang, C., Watson, D., Shterev, I., Kubo, M., Zembutsu, H., Winer, E.P., Hudis, C.A., Shulman, L.N., Nakamura, Y., Ratain, M.J., Kroetz, D.L., Cancer, B., Leukemia Group, Cox, N.J., Dolan, M.E., 2013. Integration of cell line and clinical trial genome-wide analyses supports a polygenic architecture of paclitaxel-induced sensory peripheral neuropathy. Clin. Cancer Res. 19, 491–499.

Wheeler, H.E., Wing, C., Delaney, S.M., Komatsu, M., Dolan, M.E., 2015. Modeling chemotherapeutic neurotoxicity with human induced pluripotent stem cell-derived neuronal cells. PLoS One 10, e0118020.

Wiethoff, S., Arber, C., Li, A., Wray, S., Houlden, H., Patani, R., 2015. Using human induced pluripotent stem cells (hiPSC) to model cerebellar disease: hope and hype. J. Neurogenet. 1–25.